Open Access Library Journal
2025, Volume 12, e14047
ISSN Online: 2333-9721
ISSN Print: 2333-9705

Integrating Remote Sensing and Machine Learning to Evaluate Riverbank Instability in the Akanyaru Transboundary Region

Dyna Uwambajimana[1*], Stephen Uwamahoro[1], Frank Nsimire[1], Elias Nyandwi[2], Angelique Nishyirimbere[3], Sabato Nzamwita[1], Isaac Nzayisenga[4], Stephen Mbewe[5], Bertil Nlend[6], Sèlomè Karen de Lespérance Ague[7], Katabarwa Murenzi Gilbert[8]

[1]Department of Spatial Planning, University of Rwanda, Kigali, Rwanda
[2]Centre for Geographic Information Systems and Remote Sensing, University of Rwanda, Kigali, Rwanda
[3]School of Earth Science and Engineering, Hohai University, Nanjing, China
[4]College of Geography and Remote Sensing, Hohai University, Nanjing, China
[5]Department of Geology, University of Zambia, Lusaka, Zambia
[6]Faculty of Sciences, University of Douala, Douala, Cameroon
[7]Department Laboratory of Applied Hydrology, University of Abomey-Calavi, Abomey-Calavi, Benin
[8]Department of Construction Management and Real Estate, Tongji University, Shanghai, China
Email: dynamereki@gmail.com

How to cite this paper: Uwambajimana, D., Uwamahoro, S., Nsimire, F., Nyandwi, E., Nishyirimbere, A., Nzamwita, S., Nzayisenga, I., Mbewe, S., Nlend, B., Ague, S.K. de L. and Gilbert, K.M. (2025) Integrating Remote Sensing and Machine Learning to Evaluate Riverbank Instability in the Akanyaru Transboundary Region. *Open Access Library Journal*, **12**: e14047.
https://doi.org/10.4236/oalib.1114047

Received: July 30, 2025
Accepted: September 12, 2025
Published: September 15, 2025

Abstract

Riverbank instability poses a mounting global threat, especially across East Africa's transboundary river systems, where geospatial assessments remain scarce. This study applies advanced remote sensing and machine learning regression techniques to quantify riverbank displacement along the Akanyaru River (Rwanda-Burundi) from 2004 to 2024, using Landsat and Sentinel-1 imagery, elevation data, and open-source geospatial platforms (Google Earth Engine, QGIS, Python). Key objectives include: 1) assess spatial degradation and extent of riverbank shifts, 2) forecast future river flow displacement for 2034, 3) examine the relationship between land use/land cover (LULC), slope, and flood inundation, and 4) evaluate buffer zone protection policies and socioeconomic effects on adjacent communities Results reveal marked spatial variation, including predicted reversal at Location B (−1203.5 m), persistent erosion at Location A (+950 m), and relative stability at Location C (+517 m). Agricultural encroachment and low-slope terrain exacerbate degradation and flooding, leading to 400.69 hectares of cropland loss and ecosystem service depletion valued at $2.23 million. Despite formal environmental laws in both Rwanda and Burundi, enforcement remains weak due to vague buffer zone boundaries and minimal community engagement. The study recommends deploying sat-

ellite-based early warning systems, revising buffer policies, promoting agroforestry near riparian zones, and integrating high-resolution socioeconomic data into future modelling. These insights strengthen riverbank resilience strategies and advance Sustainable Development Goals 13 (Climate Action) and 15 (Life on Land).

Subject Areas

Hydrology and Water Resources, Remote Sensing, Environmental Sciences

Keywords

Riverbank Instability, Akanyaru River, Linear Regression Model, Supervised Classification, Ecosystem Services Loss, Rwanda and Burundi

1. Introduction

The preservation of biodiversity, ecological balance, and human activity all depend primarily on surface water [1]. It includes wetlands, lakes, rivers, and reservoirs, all vital water resources for household, industrial, and agricultural purposes. Comprising surface water bodies and their interdependent drainage networks, the hydrological network is extremely dynamic and impacted by terrain, land cover, land use, and climatic change [2]. These factors shape river flow patterns, sediment transport, and erosion processes, ultimately impacting riverbank stability. Riverbank instability is characterized by erosion, mass failure, high saturation, and structural weakening due to both natural and anthropogenic factors is including deforestation, agricultural expansion, sand mining, construction near riverbanks, and poor land-use practices [3].

Riverbank instability has been studied since engineers in colonial areas, such as India, started recording significant erosion during infrastructure projects in the late 19th and early 20th centuries [4]. Powerful natural forces that might destabilise riverbanks were previously highlighted by the major bank collapses triggered by the 1811-1812 Mississippi River earthquakes [5]. Another notable event was the disastrous Yellow River floods in China in 1931, which led to widespread bank collapse and devastation [6]. By the middle of the 20th century, nations like Bangladesh had started creating workable protection measures like revetments based on extensive research on river dynamics [7].

Major rivers in East Africa, including the Rufiji River in Tanzania, the Akagera River in Rwanda and Uganda, and the Tana River in Kenya, are greatly impacted by riverbank instability. The longest river in Kenya, the Tana, is essential for irrigation and the production of hydroelectric power, but upstream development projects like the High Grand Falls Dam are endangering its stability by lowering downstream water flow and affecting agriculture in the lower catchment region [8]. Concerns over downstream flow and hydropower generation have been raised by the Akagera River's recent avulsion near Lake Rweru, which changed its chan-

nel [9]. The ecological health of Tanzania's Rufiji River and the lives of the populations that depend on its supplies are both impacted by sedimentation and changes in land use [10].

Riverbank instability is a major issue, particularly in Rwanda's Nyabarongo–Akagera system. Nearly half of Rwanda's land is at high risk of erosion, and the country loses over 595 million tons of topsoil yearly as a result [11]. Communities who live close to rivers lose clean water and agriculture, and occasionally they are forced to relocate because their property becomes unhealthy [12]. Heavy rains in May 2023 exacerbated the impact of unstable riverbanks by causing floods and landslides with 131 people losing their lives and close on 6000 homes destroyed [13].

A crucial environmental and socioeconomic issue is riverbank instability, especially in transboundary river basins with little coordinated management. No exist studies have used geospatial methods and predictive modelling to evaluate the riverbank instability of the Akanyaru River, which is shared by Rwanda and Burundi, despite its ecological and livelihood significance. This research fills that gap by applying remote sensing and machine learning techniques to 1) assess riverbank extent changes and degradation from 2004 to 2024 and predict future river flow displacement in 2034; 2) analyse the influence of geomorphological features, river flow dynamics, and their impacts on surrounding communities; and 3) evaluate the effectiveness of policy implementation in river buffer zone management. The results will assist evidence-based policymaking, provide crucial guidance on transboundary river management, and help accomplish SDGs 13 (Climate Action) and 15 (Life on Land) [14].

2. Materials and Methods

This study evaluated LULC changes along the Akanyaru River from 2004 to 2024, the impact on communities, and riverbank instability using remote sensing and machine learning approaches. Riverbank the digitization was conducted using Google Earth Pro, which made it possible to manually trace historical river the placement for a few selected years to verify and contrast them with extents determined by satellite. LULC and riverbank extent were mapped using Landsat, while cloudy circumstances enabled the detection of flooded areas using Sentinel-1 radar imagery. Google Earth Engine was used for image processing and categorization, and regression-based machine learning models in Jupyter Notebook were utilized for predicting river flow displacement for 2034. The research methodology used in this study is illustrated in **Figure 1**.

2.1. Description of the Study Area

The Akanyaru River is a transboundary river that runs along the common border between Rwanda and Burundi in East-Central Africa [15]. It rises to an elevation of about 2450 meters in Burundi and 2300 meters in Southern Rwanda in the highlands of both countries. Then flows north to join the Nyabarongo River at

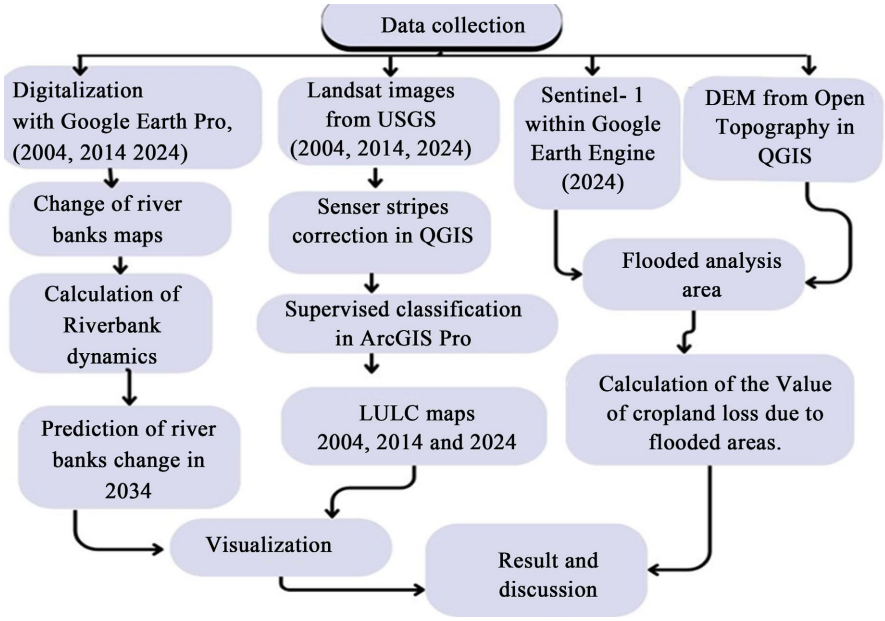

Figure 1. Study framework.

Bugesera in Eastern Rwanda, where it becomes the Akagera River, the biggest tributary of Lake Victoria [16]. The approximate coordinates of the river are 2.07504˚S, 30.018929˚E, and the size of its upstream watershed is around 2650 meters. This area has an intertropical climate with two distinct rainy seasons, from March to May and mid-September to mid-December. The upstream regions receive an average of 1200 mm of rainfall annually, while the marshes receive 800 mm. In addition to papyrus marshes and swamp woods in tributary valleys, the vegetation consists of species including Phoenix reclinate, Ficus verrucous, and Acacia polyantha. With more than 60 bird species identified in the marshes, biodiversity is abundant. Fifteen administrative cells along or close to the Akanyaru River were chosen for this investigation. There are eight cells in Rwanda (Gitega, Mukiza, Mukomacara, Nyabisagara, Rubona, Runyinya, Umubanga, and Buziragahama) and seven in Burundi (Cahi, Gitwa, Martyazo, Nyabikene, Nyamurenge, Nyunzwe, and Rukurazo) (**Figure 2**). These cells were selected due to their closeness to the riverbanks and discernible changes in land use or riverine conditions during the previous few decades.

2.2. Data Acquisition and Pre-Processing

2.2.1. Secondary Data Collection (Desk-Based)

Sentinel-1 data (10 m resolution) were used for 2024, while Landsat imagery (30 m) covered 2004 and 2014. Each image had ≤ 5% cloud cover and was processed in Google Earth Engine. Elevation data (10 m DEM) were obtained via QGIS's OpenTopography plugin for terrain and slope analysis. Administrative boundaries from DIVA-GIS defined the study region (**Table 1**). We selected three decadal benchmarks—2004, 2014, and 2024—to balance data quality, processing efficiency, and alignment with major hydrological and policy milestones

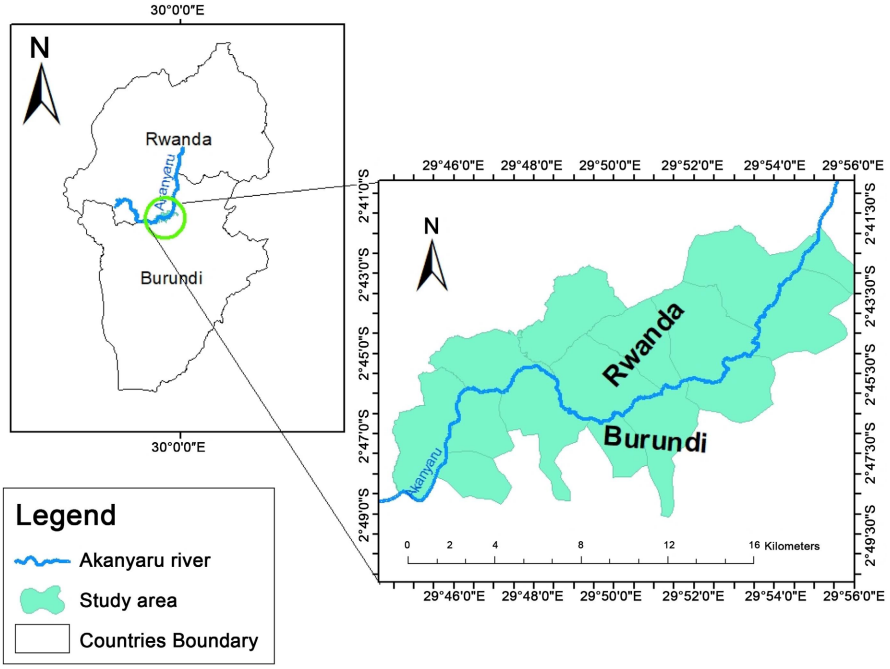

Figure 2. Map of study area (Source: Authors, 2025).

(pre-intensification, buffer-zone policy rollout, current baseline). Future research should integrate intermediate or annual imagery to capture non-linear channel shifts and short-term LULC dynamics.

Table 1. Data list.

Category	Name	Description	Access Method/Source	Timeframe
Satellite Imagery	Landsat	30m resolution for land cover classification	Processed in Google Earth Engine (May 2025)	2004, 2014
	Sentinel-2	10m resolution for land cover classification	Processed in Google Earth Engine (May 2025)	2024
Auxiliary Data	Elevation	10m resolution DEM	OpenTopography DEM Downloader (QGIS 3.34)	-
	Administrative Boundaries	Vector shapefiles for Rwanda and Burundi	DIVA-GIS (22 April 2025)	-

2.2.2. Remotely Sensed Data (Satellite Imagery)

This study used Sentinel-1 SAR Ground Range Detected (GRD) products available on Google Earth Engine, and all satellite imagery was reprojected to WGS 1984/UTM Zone 35S. Standard preprocessing (thermal noise removal, radiometric calibration, terrain correction) was executed in GEE. Only the final map layouts, supervised land-cover classification, and cosmetic adjustments were performed in ArcGIS Pro 3.5.1. Table 2 provides a summary of the Landsat imagery's primary attributes, such as sensor type, spatial resolution, and acquisition times.

Table 2. Characteristics of Landsat and sentinel-1 data used for the Akanyaru river study.

Mission	Sensor	Acquisition Date	Product Level	Path/Row	Resolution
Landsat 7	ETM+	23-Sep-2004	L2SP	172/062	30 m
Landsat 7	ETM+	02-Aug-2014	L2SP	172/062	30 m
Landsat 9	OLI	24-Nov-2021	L2SP (SR)	172/062	10 m
Sentinel-1	C-SAR	14-Sep-2024	Level-1 GRD	—	10 m

The land use and land cover (LULC) patterns of the study region were analysed using satellite imagery. In particular, the Scan Line Corrector (SLC) issue that affected Landsat 7 images was addressed by using "Raster Analysis—Fill NoData" to fix striping and fill in missing data gaps for the 2004 and 2014 Landsat imagery [17]. For Sentinel-1, we applied a VV backscatter difference thresholding method on the SAR time-series in GEE to delineate inundated areas in 2024. By calculating VV_diff between pre- and post-monsoon acquisitions, we mapped flood extents directly from SAR backscatter. VV polarization clearly distinguishes water from dry land and has proven reliable for flood mapping [18].

2.2.3. Sampling Design and Field Data Collection

Figure 3 shows the three sample locations along the Akanyaru River that were chosen for the investigation. Located in Cell 4, Location A comprises Rukurazo, Gitwa, Umubanga, and Rubona. Location B includes Nyabikenke, Cahi, Mukiza, and Gitega. Runyinya, Nyunzwe, and Nyabisagara are all part of Location C. These sites were chosen because they are ideal for capturing all of the pertinent characteristics and phenomena covered in this study, including ecological conditions, land use changes, and riverbank dynamics.

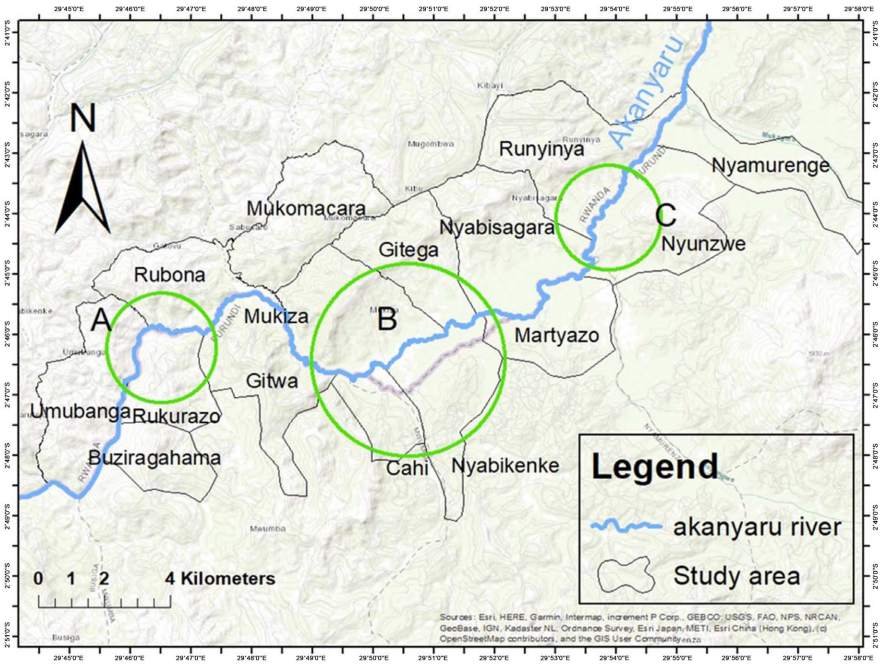

Figure 3. Sampling location map of study area.

2.3. Estimation of Ecosystem Service Value Loss Due to Flooding

This study calculated the ecosystem service value (ESV) loss due to flooding by applying the following formula:

$$\mathrm{ESV} = \sum_{i=1}^{n} \left(CA_i \times UV_i \right) \tag{1}$$

where ESV represents the total ecosystem service value in USD, CA_i is the area (in hectares) of each land use type or patch i, UV_i's the unit value assigned per hectare for each land type, and n is the number of land use patches considered [19]. By multiplying the flooded area of each land type by its respective unit value and summing across all affected land types, the study estimated the total economic loss of ecosystem services resulting from the flood event.

2.4. Python-Based Linear Regression Model for Predicting Riverbank Change in 2034

This study used a Python-based linear regression model, which can handle massive temporal datasets and provide high-accuracy predictions [20]. The Python linear regression model is a machine learning approach that models the connection between a dependent variable and one or more independent variables by fitting a linear equation to observed data [21] [22]. In this case, the dependent variable is riverbank displacement, and the independent variable is time (years since 2004) (**Table 3**). The time series data used for model training included displacement measurements from 2004, 2014, and 2024.

Table 3. River flow displacement in meter.

Sampling Location	Displacement (2004-2014)	Displacement (2014-2024)	Total Displacement (2004-2024)
A	200 m	575 m	775 m
B	1423.53 m	110 m	1533.53 m
C	537 m	527 m	1064 m

The linear model is expressed as:

$$y = mx + b \tag{2}$$

In this case, y represents the dependent variable (river flow displacement), x the independent variable (years after 2004), m the slope (time change rate), and b the y-intercept (the initial displacement m value at 2004). We were able to use this strategy to extrapolate from previous observations and forecast the river flow scenario for 2034. To assess model robustness, we conducted leave-one-out cross-validation (LOOCV). The resulting mean absolute error (MAE) was 62.4 m, and the root mean square error (RMSE) was 74.8 m. These metrics indicate strong predictive reliability. Furthermore, 95% confidence intervals were calculated for each location's 2034 forecast: Location A: 950 ± 68 m; Location B: −1203.5 ± 74 m; Location C: 517 ± 62 m. These additions provide a transparent view of model

uncertainty and support its application in forecasting riverbank dynamics within the Akanyaru transboundary region.

2.5. Accuracy Assessment

2.5.1. Confusion Matrix

We evaluated categorized maps for each study year using confusion matrices. The categorized pixels of the test samples were compared to the matrix. The producer's, user's, kappa index, and total accuracy make up the confusion matrices (**Table 3**). The percentage of samples that are properly categorized is known as overall accuracy. The LULC map's correctness, on the other hand, is the producer's accuracy as figured out by the map producer [23] [24]. These were distributed across the entire study area to capture all LULC classes kappa index assesses the level of agreement between the classifier and the test data, while the user's point of view determines the correctness of the map [24]. To ensure reproducibility and spatial representativeness, we used a stratified random sampling strategy across all 15 administrative cells. A total of 233 reference points for 2004, 280 for 2014, and 218 for 2024 were collected and distributed across four LULC classes: waterbodies, wetlands, agriculture, and vegetation. These validation points were interpreted using high-resolution imagery in Google Earth Pro and were independent from the training samples used for classification. The spatial distribution captured upstream, midstream, and downstream zones to reflect geographic variability.

This equation could potentially be used to decide the kappa index:

$$K = \frac{\left(f_0 - f_E\right)}{\left(N - f_E\right)} \tag{3}$$

where f_E is the number of agreements that are by chance, f_0 is the number of observed agreements, and N is the total number of observations [25]. The Kappa coefficient reflects how closely the classified results agree with reference data beyond random chance than the one predicted by chance (represented by f_E), and K = 1 if the observations are completely in accord [25]. **Table 4** presents the classification performance for each year and location, highlighting strong consistency between classified outputs and reference data. As finding by Elhadi Adam, 2023, These numbers are significantly higher than the 85% is good accuracy [25].

Table 4. Accuracy assessment results for LULC classification (2004, 2014 and 2024).

	Year	Waterbodies	Wetland	Agriculture	Vegetation	Overall Accuracy (%)	Kappa Coefficient
2024	Reference total	48	70	60	40	98.41	0.964
	Classified total	50	72	60	40		
	Correctly classified	48	70	60	35		
	UA (%)	96	97.22	100	87.5		
	PA (%)	100	96.88	100	87.5		

Continued

	Reference total	60	80	80	60		
	Classified total	60	77	80	60		
2014	Correctly classified	40	72	77	53	92.11	0.889
	UA (%)	100	93.51	96.25	88.33		
	PA (%)	66.67	93.55	96.08	88.46		
	Reference total	48	70	65	50		
	Classified total	48	70	50	51		
2004	Correctly classified	48	58	43	34	84.03	0.751
	UA (%)	100	82.86	86	66.67		
	PA (%)	100	82.61	93.48	68		

2.5.2. Validation of LULC

LULC classification accuracy was evaluated using Google Earth Pro v7.3 with high-resolution, time-series satellite images [26]. Using georeferenced data from many years, to validate the classification results, high-resolution satellite images from Google Earth Pro were visually compared with historical datasets to assess alignment with real-world features. This method worked especially well for locating slum areas and tracking how they changed over time [27]. The spatial accuracy of the categorization findings was evaluated by superimposing current and historical datasets. By ensuring that the categorized maps properly depicted the real circumstances on the ground, this validation method offered a strong basis for verifying the outputs consistency and dependability [28]. The accuracy evaluation, which is shown in **Table 3**, validates the dependability and spatial precision of the LULC analysis by showing the degree of agreement between the classified data and reference imagery [29].

2.5.3. Flood Extent Validation Using VV_diff Thresholding

Flood extent validation was conducted using the VV backscatter intensity recorded before the flood event thresholding method, which detects inundated areas by analyzing changes in radar backscatter intensity from Sentinel-1 VV polarization data. This approach relies on the pixel-wise difference between two temporally distinct SAR acquisitions:

$$VV_{diff} = VV_{pre} - VV_{post} \tag{4}$$

Flooded surfaces typically exhibit a marked reduction in backscatter due to specular reflection from smooth water bodies, resulting in high VV pre values. A threshold of 2.0 dB was applied to classify pixels as flooded. Validation was performed using reference data and evaluated through standard metrics Overall Accuracy (OA), Precision, Recall, F1 Score, and Kappa Coefficient as defined below:

$$\text{F-Score} = \frac{TP}{TP + FP + FN} \tag{5}$$

$$\mathrm{OA}(\%) = \frac{\mathrm{TP} + \mathrm{TN}}{\mathrm{TP} + \mathrm{FN} + \mathrm{FP} + \mathrm{TN}} \tag{6}$$

$$K = \frac{P_o - P_e}{1 - P_e} \tag{7}$$

$$P_o = \frac{\mathrm{TP} + \mathrm{TN}}{\mathrm{T}} \tag{8}$$

$$P_e = \frac{(\mathrm{TP} + \mathrm{FP}) * (\mathrm{TP} + \mathrm{FN}) + (\mathrm{TN} + \mathrm{FP}) * (\mathrm{TN} + \mathrm{FN})}{\mathrm{T}^2} \tag{9}$$

where, true positives (TP) refer to flooded pixels that were correctly identified by the model, while true negatives (TN) are non-flooded pixels that were accurately classified as such. False positives (FP) represent pixels that were incorrectly labeled as flooded, and false negatives (FN) are actual flooded pixels that the model failed to detect. For the kappa coefficient (K), P_o is the observed agreement, P_e is the expected agreement, and T is the total number of pixels in the flood map, which is (TP + FN + FP + TN) [30] (**Table 5**).

Table 5. Validation results for 2024 flood event.

Date	TP	TN	FP	FN	OA	Precision	Recall	F1 Score	Kappa
2024	544	3832	0	589	0.88	1.00	0.48	0.65	0.59

3. Results and Discussion

3.1. Riverbank Extent Changes and Degradation Assessment

A thorough examination of the Akanyaru River's riverbank modifications from 2004 to 2024 shows notable changes at the chosen sampling sites. Approximately 200 meters were shifted by the riverbank at place A, 1423.53 meters at location B, and 537 meters at location C between 2004 and 2014. Additional displacement was noted at locations A, B, and C between 2014 and 2024: 575 meters, 110 meters, and 527 meters, respectively. Upstream, a 2004-formed alluvial lake significantly grew by 2014, changing the river's width and flow direction. **Figure 4** provides a vivid illustration of these spatial differences by comparing the locations of riverbanks during the three research years and highlighting the regions most impacted by channel movement and river flow deterioration.

Similar patterns of riverbank degradation in transboundary rivers have been reported worldwide. Strong monsoonal rainfall and sediment-rich flows have led to significant erosion and deposition in the Ganges-Brahmaputra-Meghna (GBM) basin between India and Bangladesh, especially along the Jamuna River, where riverbanks have moved several kilometres since the 1970s, uprooting thousands of people every year [31]. Sea level rise brought on by climate change and decreased dry-season discharge make these effects much worse [32]. In other places, channel engineering and sediment dynamics have changed the flow of the Oder River (Poland–Germany) and the Rio Grande (USA-Mexico), necessitating bilateral management collaboration [33] [34].

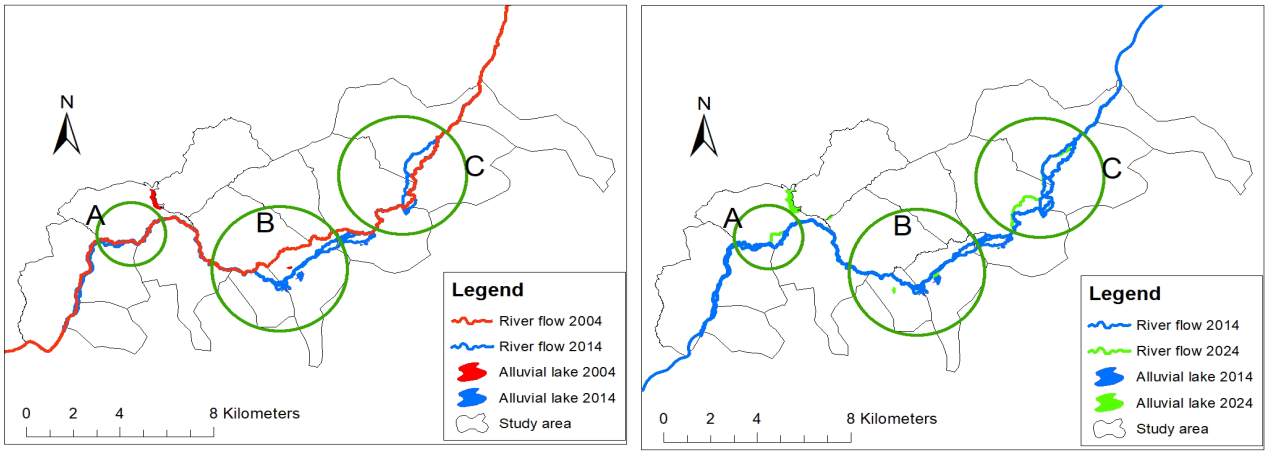

Figure 4. Riverflow change from 2004 to 2024.

Similar bank retreat is seen in the Zambezi and Senegal Rivers in Africa as a result of agricultural growth and dam activities, upsetting sediment regimes and endangering local livelihoods [35] [36]. These global instances are reflected in the development of the Akanyaru River, highlighting the pressing need for coordinated watershed management. Stabilising riverbanks and establishing long-term ecological and social resilience can be achieved through the implementation of adaptive engineering solutions, the restoration of riparian buffers, and the promotion of sustainable land-use practices [37] [38].

3.2. Predict Future River Flow Displacement in 2034

Since observed patterns, future displacement for the 2024-2034 period was forecast using linear regression modelling. With an expected displacement of 950 meters, the model predicts ongoing riverbank migration at Location A. Location B, on the other hand, has a reversal pattern with a projected negative displacement of –1203.5 meters (return to the old path) (**Figure 5**), suggesting that it may have reoccupied its previous course, perhaps as a result of geomorphic correction or sediment deposition. The expected displacement at Location C is just 517 meters, indicating a channel system that is comparatively stable. These results highlight the necessity of location-specific river management plans, especially in regions that are undergoing fast geomorphological change or high levels of instability.

3.3. The Impact of LULC on Riverbank Stability

The waterbody area along the Akanyaru River has grown over the past 20 years, as seen by the maps from 2004, 2014, and 2024, which also show a rise in the river's surface extent. This growth is especially apparent between 2014 and 2024. However, there is a noticeable increase in agricultural encroachment close to the riverbanks at the same time as the growth of waterbodies. Although it has somewhat decreased by 2024, agricultural land still dominates the surrounding environment, particularly in 2004 and 2014, and is still common at river borders (**Figure 6**).

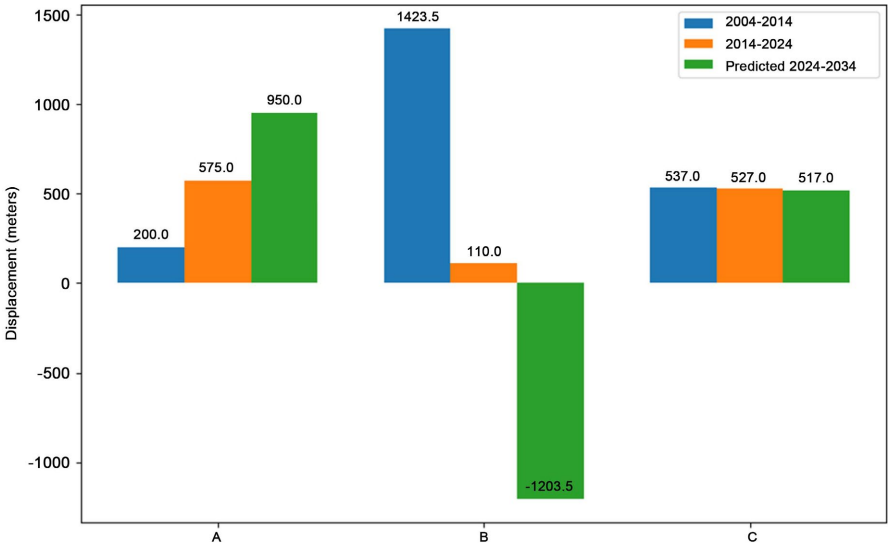

Figure 5. River flow displacement in 2034.

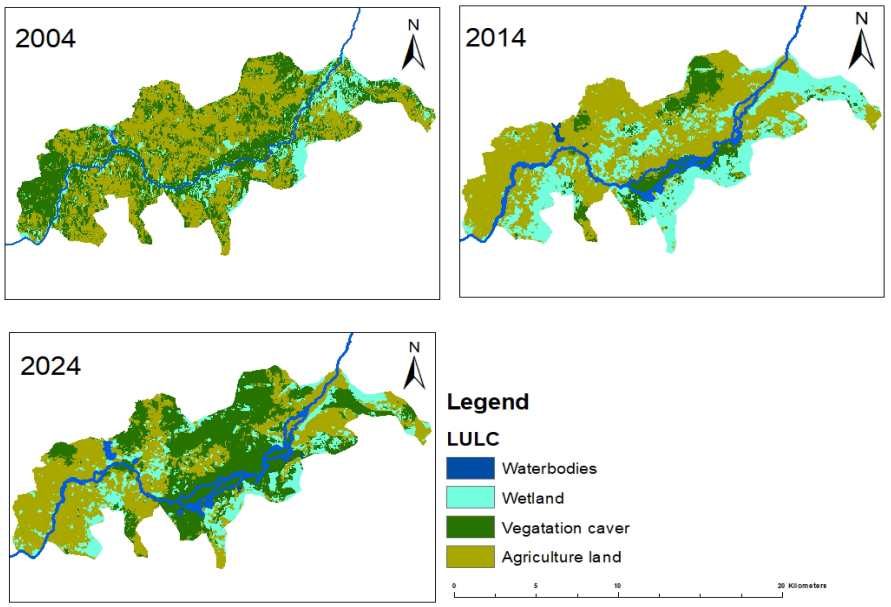

Figure 6. LULC maps (2004, 2014, 2024).

Similar results have been shown in various river systems across the world. Zaimes and Camporees point out that through soil disturbance and plant clearance, agricultural growth close to riparian zones frequently speeds up riverbank erosion [39] [40]. Extensive farming along rivers in East Africa has been linked in studies [41] to increased bank instability and sedimentation, which in turn influence water quality and flow regimes. Williams (2016) adds that rather than being a sign of beneficial hydrological change, an increase in river surface area may be a sign of channel widening brought on by erosion [42]. These studies collectively corroborate the notion that agricultural encroachment and riverbank degradation are closely related processes that jeopardise river health, underlining the necessity

of maintaining riparian vegetation and controlling land use near to rivers.

3.4. The Role of Topography in Influencing Flooding Patterns

Slope values around zero in the Akanyaru River basin's topographic study show that low-lying regions are most affected by floods. According to the spatial distribution of slope data, areas with flat terrain especially those that are close to a river channel—are more vulnerable to floods [43]. These regions match those that prior hydrological evaluations have shown to be flood prone. On the other hand, upland areas with steeper slopes are less likely to flood because surface runoff tends to drain away from them more rapidly. Thus, it is evident from the slope map (**Figure 7**) that the lowland floodplains around the Akanyaru River are where flood episodes are concentrated.

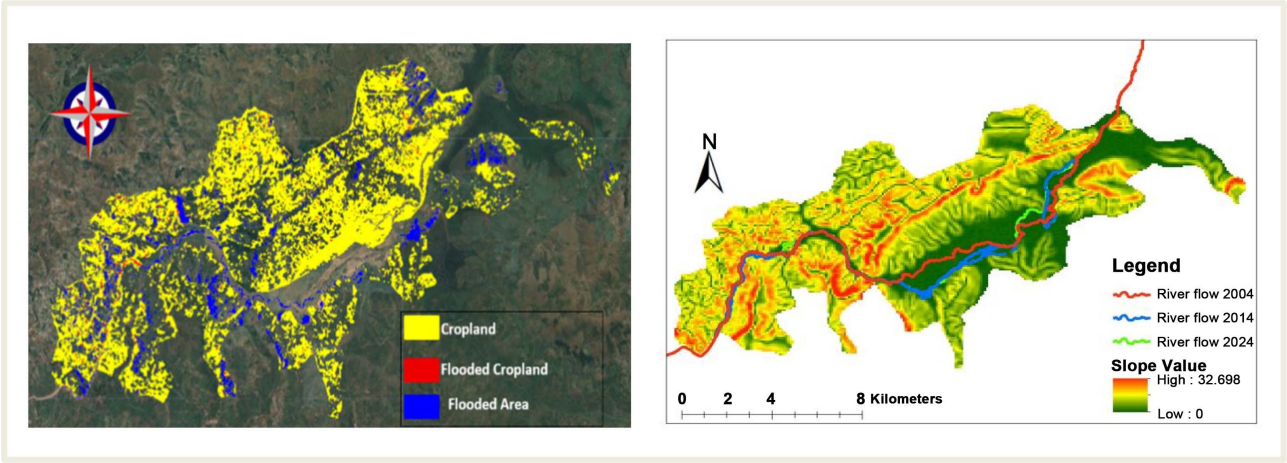

Figure 7. Map of flooded area and slope.

The important significance of topography in flood dynamics has been shown by several research. Olang and Fürst (2011) state that areas with slopes less than 2% are more susceptible to flooding because of their inadequate drainage capabilities [44]. In a similar vein, Das and Pardeshi's (2018) study shows that lowland floodplains are natural locations for runoff collecting, particularly when paired with upstream land disturbances and high rainfall [45]. Studies like those of Di Baldassarre (2012) highlight how topography, land use, and climate interact to shape flood risk in Sub-Saharan Africa, demonstrating that flat terrain with intensive land use significantly enhances the extent and intensity of floods [46]. In order to increase resilience in vulnerable riverine areas, our findings highlight the need of using slope data in flood hazard mapping and planning.

3.5. The Socio-Economic Implications of Akanyaru Riverbank Instability

3.5.1. On Local Livelihoods Due to These Environmental Changes

The findings show that environmental changes in the study region have a major socioeconomic influence on local livelihoods. About 85% of the land is covered

by agriculture, highlighting the community's heavy reliance on farming for both economic creation and subsistence. A significant amount of productive agricultural land was lost as 400.69 hectares **Table 6** of the projected 5244.17 hectares of total farmland area were discovered to be inundated. As a result, there are now 4843.48 hectares of usable agriculture left, which poses major risks to food security and undermines the principal source of income for many people.

Table 6. Estimated ecosystem service value loss due to flooded cropland in the study area.

Equivalent ecosystem	Estimated ES unit value (USD/ha)	Flooded cropland area (ha)	Estimated ESV Loss (USD)
Cropland	5567	400.69	2230263.23

Based on a unit value of USD 5567 per hectare [19], the flooded cropland shown in **Figure 7** is estimated to have caused an ecosystem service value loss of USD 2230263.23, which also highlights the direct impact on farmers and signals broader vulnerabilities within the local economy, especially in a region heavily dependent on agriculture. These findings highlight the urgent need for integrated land-use planning, effective disaster risk reduction strategies, and the adoption of climate-resilient agricultural practices to protect and strengthen the socio-economic wellbeing of the affected communities.

3.5.2. Policy Assessment for Buffer Zone Protection

Burundi's Environmental Code of 2011 and Rwanda's Environment Law No. 48/2018 are two examples of legislative frameworks that have been implemented to safeguard riverbanks and buffer zones, but they are not being effectively enforced, especially in rural and transboundary areas. Buffer zone infractions, including habitation, farming, and informal activities, continue in Rwanda despite institutional frameworks such as REMA and RLMUA because of a lack of technical expertise, poor local administration, and insufficient finance [47] [48].

Similar to this, environmental governance in Burundi is essentially nonfunctional due to inadequate interministerial cooperation and persistent political unrest, with little to no monitoring of encroachment on protected wetlands [49]. The lack of physically defined buffer zone boundaries in both nations further undermines enforcement efforts by leaving local populations unsure of the boundaries of the legal buffer zones [50]. Because of this, buffer zone degradation persists even in the face of official regulations.

The lack of local community involvement in buffer zone planning and enforcement is another important factor contributing to policy failure in both countries. Often, buffer zone regulations are seen as top-down impositions that disregard customary land use rights and community livelihoods [51]. For instance, attempts to enforce waterbody protection in Burundi have resulted in the forced eviction of smallholder farmers without just compensation or legal recourse, causing social unrest and eroding confidence in state institutions [49] and in Rwanda, despite more

formalised land tenure, conflicts nonetheless occur when local farmers are penalised for cultivating historically communal lands that are now protected [52] [53].

3.6. Limitations

The accuracy and generalizability of this study's findings are subject to several limitations. First, vertical inaccuracies in the digital elevation model (DEM), estimated at approximately ±2.5 meters. Second, the need to apply SLC-off gap-filling to Landsat 7 imagery (2004-2014) may introduce minor spatial artifacts that affect land cover interpretation. Third, despite filtering for cloud cover below 5%, residual cloud contamination may obscure certain LULC features, particularly in wetland zones. Lastly, policy-related data on buffer zone enforcement are derived from publicly available documents, which may not fully capture informal land tenure systems, community perspectives, or on-the-ground implementation realities. These limitations underscore the importance of future studies incorporating field-based validation, higher-resolution datasets, and participatory policy assessments to enhance reliability and contextual relevance.

4. Conclusion and Recommendations

This research applied geospatial analysis, land use/land cover (LULC) assessment, and predictive modelling tools to examine the spatiotemporal dynamics of riverbank alterations along the Akanyaru River between 2004 and 2024. Significant riverbank instability was found in the data, with displacement in some places surpassing 1423.53 meters, especially in locations with steep slopes and little vegetative cover.

Significant wetlands and natural vegetation conversion to agricultural land was shown by LULC research, which has exacerbated erosion and sediment deposition. In accordance with the established spatial patterns of flood susceptibility, topographic evaluations revealed that places with low slope values around zero in the Akanyaru River basin's topographic analysis validate that low-lying zones are most impacted by floods. Local livelihoods suffered as a result of the anticipated loss of 400.69 hectares of crops.

Using linear regression modelling, predictions for 2024-2034 showed that the river will continue to migrate at Location A (950 m), reverse its flow direction at Location B (–1203.5 m), return to its original path, and be relatively stable at Location C (517 m). These variances highlight the significance of regional approaches to riverbank management.

Burundi's 2011 Environmental Code and Rwanda's Environment Law No. 48/2018 are two examples of existing environmental legislation. However, enforcement remains lax. Efforts to safeguard riverbanks are nevertheless hampered by a lack of community involvement, inadequate technical ability, inadequate local administration, and unclear buffer lines.

This research establishes a basis for integrated riverbank management by connecting topographic vulnerability, land use patterns, and policy difficulties with

GIS information. It helps achieve Sustainable Development Goals (SDGs) 13 (Climate Action) and 15 (Life on Land) by providing data-driven insights to assist ecosystem conservation and climate resilience in transboundary river systems.

To address the challenges identified in this study and advance the sustainable management of the Akanyaru River, several key strategies are recommended. First, it is essential to strengthen monitoring and restoration efforts through a continuous program that integrates field-based observations with satellite data, enabling the early detection of erosion and riverbank deterioration. Second, promoting sustainable land use activities—such as agroforestry and conservation agriculture—in areas adjacent to the riverbanks is crucial. This must be coupled with stricter enforcement of existing buffer zone regulations to prevent harmful encroachment. Third, enhancing institutional capacity and revisiting current riparian land-use policies will help align governance frameworks with evolving environmental challenges. Finally, future research should adopt a basin-wide approach using high-resolution geospatial datasets and socioeconomic variables. This integrated methodology will improve predictive accuracy and support targeted conservation and modeling of riverbank stability.

Acknowledgements

We sincerely thank everyone who contributed to the success of this research.

Conflicts of Interest

The authors declare no conflicts of interest.

References

[1] Singh, S., Kumar, P., Parijat, R., Gonengcil, B. and Rai, A. (2024) Establishing the Relationship between Land Use Land Cover, Normalized Difference Vegetation Index and Land Surface Temperature: A Case of Lower Son River Basin, India. *Geography and Sustainability*, **5**, 265-275. https://doi.org/10.1016/j.geosus.2023.11.006

[2] Gao, H., Sabo, J.L., Chen, X., Liu, Z., Yang, Z., Ren, Z., *et al.* (2018) Landscape Heterogeneity and Hydrological Processes: A Review of Landscape-Based Hydrological Models. *Landscape Ecology*, **33**, 1461-1480. https://doi.org/10.1007/s10980-018-0690-4

[3] Duong Thi, T. and Do Minh, D. (2019) Riverbank Stability Assessment under River Water Level Changes and Hydraulic Erosion. *Water*, **11**, Article 2598. https://doi.org/10.3390/w11122598

[4] D'Souza, R. (2015) Drainage, River Erosion, and Chaurs: An Environmental History of Land in Colonial Eastern India. *Nehru Memorial Museum and Library Occasional Paper*: *History and Society*, **84**, 22.

[5] Street, R. and Nuttli, O. (1984) The Central Mississippi Valley Earthquakes of 1811-1812. *Proceedings of the Symposium on "The New Madrid Seismic Zone"*, Reston, 26 November 1984, 33-63.

[6] Courtney, C. (2018) The Nature of Disaster in China: The 1931 Yangzi River Flood. Cambridge University Press. https://doi.org/10.1017/9781108278362

[7] Oberhagemann, K., Haque, A.M.A. and Thompson, A. (2020) A Century of

Riverbank Protection and River Training in Bangladesh. *Water*, **12**, Article 3018. https://doi.org/10.3390/w12113018

[8] Goswami, S. (2017) Kenya's Tana River Delta under Threat from Development Projects. Down to Earth. https://www.downtoearth.org.in/environment/kenya-s-tana-river-delta-under-threat-from-development-projects-58267

[9] Munyaneza, O., Ndayisaba, C., Wali, U.G., Mulungu, D.M.M. and Dulo, S.O. (2011) Integrated Flood and Drought Management for Sustainable Development in the Kagera River Basin. *Nile Water Science Engineering Journal*, **4**, 60-70.

[10] Kimambo, O.N., Mbungu, W., Massawe, G.D., Hamad, A.A. and Ligate, E.J. (2023) Rapid Environmental Flow Assessment for Sustainable Water Resource Management in Tanzania's Lower Rufiji River Basin: A Scoping Review. *Heliyon*, **9**, e22509. https://doi.org/10.1016/j.heliyon.2023.e22509

[11] Karamage, F., Zhang, C., Ndayisaba, F., Shao, H., Kayiranga, A., Fang, X., *et al.* (2016) Extent of Cropland and Related Soil Erosion Risk in Rwanda. *Sustainability*, **8**, Article 609. https://doi.org/10.3390/su8070609

[12] Douglas, I., Alam, K., Maghenda, M., Mcdonnell, Y., Mclean, L. and Campbell, J. (2008) Unjust Waters: Climate Change, Flooding and the Urban Poor in Africa. *Environment and Urbanization*, **20**, 187-205. https://doi.org/10.1177/0956247808089156

[13] ReliefWeb (2023) Rwanda: Floods and Landslides—May 2023. ReliefWeb. https://reliefweb.int/disaster/fl-2023-000064-rwa

[14] United Nations (2025) The 17 Goals | Sustainable Development. United Nations Sustainable Development. https://sdgs.un.org/goals

[15] Deak, M. (2023) Akanyura River—WorldAtlas. WorldAtlas. https://www.worldatlas.com/rivers/akanyura-river.html

[16] Benjamin, G. (2015) Assessment of Micro to Small Hydropower Potential Sites of Nyabarongo River Basin of Rwanda. Ph.D. Thesis, Arba Minch University.

[17] Gilbert, K.M. and Shi, Y. (2023) Slums Evolution and Sustainable Urban Growth: A Comparative Study of Makoko and Badia-East Areas in Lagos City. *Sustainability*, **15**, Article 14353. https://doi.org/10.3390/su151914353

[18] Vekaria, D., Chander, S., Singh, R.P. and Dixit, S. (2022) A Change Detection Approach to Flood Inundation Mapping Using Multi-Temporal Sentinel-1 SAR Images, the Brahmaputra River, Assam (India): 2015-2020. *Journal of Earth System Science*, **132**, Article No. 3. https://doi.org/10.1007/s12040-022-02020-x

[19] Mugiraneza, T., Ban, Y. and Haas, J. (2019) Urban Land Cover Dynamics and Their Impact on Ecosystem Services in Kigali, Rwanda Using Multi-Temporal Landsat Data. *Remote Sensing Applications*: *Society and Environment*, **13**, 234-246. https://doi.org/10.1016/j.rsase.2018.11.001

[20] Ramzan, M., Saqib, Z.A., Hussain, E., Khan, J.A., Nazir, A., Dasti, M.Y.S., *et al.* (2022) Remote Sensing-Based Prediction of Temporal Changes in Land Surface Temperature and Land Use-Land Cover (LULC) in Urban Environments. *Land*, **11**, Article 1610. https://doi.org/10.3390/land11091610

[21] Géron, A. (2019) Hands-On Machine Learning with Scikit-Learn, Keras, and Tensor Flow: Concepts, Tools, and Techniques to Build Intelligent Systems. 2nd Edition, O'Reilly Media.

[22] James, G., Witten, D., Hastie, T. and Tibshirani, R. (2013) An Introduction to Statistical Learning. Springer.

[23] Kamusoko, C. (2019) Improving Image Classification. In: Kamusoko, C., Ed., *Remote Sensing Image Classification in R*, Springer, 155-181. https://doi.org/10.1007/978-981-13-8012-9_5

[24] Adam, E., Masupha, N.E. and Xulu, S. (2023) Spatial Assessment and Prediction of Urbanization in Maseru Using Earth Observation Data. *Applied Sciences*, **13**, Article 5854. https://doi.org/10.3390/app13105854

[25] Mosammam, H.M., Nia, J.T., Khani, H., Teymouri, A. and Kazemi, M. (2017) Monitoring Land Use Change and Measuring Urban Sprawl Based on Its Spatial Forms. *The Egyptian Journal of Remote Sensing and Space Sciences*, **20**, 103-116. https://doi.org/10.1016/j.ejrs.2016.08.002

[26] Farhan, M., Wu, T., Amin, M., Tariq, A., Guluzade, R. and Alzahrani, H. (2024) Monitoring and Prediction of the LULC Change Dynamics Using Time Series Remote Sensing Data with Google Earth Engine. *Physics and Chemistry of the Earth, Parts A/B/C*, **136**, Article ID: 103689. https://doi.org/10.1016/j.pce.2024.103689

[27] Haining, R.P. (2009) The Nature of Georeferenced Data. In: Fischer, M. and Getis, A., Eds., *Handbook of Applied Spatial Analysis*, Springer, 197-217. https://doi.org/10.1007/978-3-642-03647-7_12

[28] Amini, S., Saber, M., Rabiei-Dastjerdi, H. and Homayouni, S. (2022) Urban Land Use and Land Cover Change Analysis Using Random Forest Classification of Landsat Time Series. *Remote Sensing*, **14**, Article 2654. https://doi.org/10.3390/rs14112654

[29] Foody, G., Pal, M., Rocchini, D., Garzon-Lopez, C. and Bastin, L. (2016) The Sensitivity of Mapping Methods to Reference Data Quality: Training Supervised Image Classifications with Imperfect Reference Data. *ISPRS International Journal of Geo-Information*, **5**, Article 199. https://doi.org/10.3390/ijgi5110199

[30] Belay, H., Melesse, A.M., Tegegne, G. and Kassaye, S.M. (2025) Flood Inundation Mapping Using the Google Earth Engine and HEC-RAS under Land Use/land Cover and Climate Changes in the Gumara Watershed, Upper Blue Nile Basin, Ethiopia. *Remote Sensing*, **17**, 1283. https://doi.org/10.3390/rs17071283

[31] Freihardt, J. and Frey, O. (2023) Assessing Riverbank Erosion in Bangladesh Using Time Series of Sentinel-1 Radar Imagery in the Google Earth Engine. *Natural Hazards and Earth System Sciences*, **23**, 751-770. https://doi.org/10.5194/nhess-23-751-2023

[32] Bricheno, L.M., Wolf, J. and Sun, Y. (2021) Saline Intrusion in the Ganges-Brahmaputra-Meghna Megadelta. *Estuarine, Coastal and Shelf Science*, **252**, Article ID: 107246. https://doi.org/10.1016/j.ecss.2021.107246

[33] Flores, A.A. (2022) Rivers as International Borders: A Comparison of How Social-Political Factors Have Impacted Natural Resources in the Usumacinta River Basin and Rio Grande River Basin within the Context of Climate Change. Ph.D. Thesis, Texas A&M University-San Antonio.

[34] Tanzi, A. and Arcari, M. (2021) The United Nations Convention on the Law of International Watercourses: A Framework for Sharing. Brill.

[35] Sall, M., Poussin, J., Bossa, A.Y., Ndiaye, R., Cissé, M., Martin, D., *et al.* (2020) Water Constraints and Flood-Recession Agriculture in the Senegal River Valley. *Atmosphere*, **11**, Article 1192. https://doi.org/10.3390/atmos11111192

[36] Khan, O., Mwelwa-Mutekenya, E., Crosato, A. and Zhou, Y. (2014) Effects of Dam Operation on Downstream River Morphology: The Case of the Middle Zambezi River. *Proceedings of the Institution of Civil Engineers—Water Management*, **167**, 585-600. https://doi.org/10.1680/wama.13.00122

[37] Kondolf, G.M., Gao, Y., Annandale, G.W., Morris, G.L., Jiang, E., Zhang, J., *et al.* (2014) Sustainable Sediment Management in Reservoirs and Regulated Rivers: Expe-

riences from Five Continents. *Earth's Future*, **2**, 256-280. https://doi.org/10.1002/2013ef000184

[38] Wohl, E., Lane, S.N. and Wilcox, A.C. (2015) The Science and Practice of River Restoration. *Water Resources Research*, **51**, 5974-5997. https://doi.org/10.1002/2014wr016874

[39] Zaimes, G.N. and Schultz, R.C. (2015) Riparian Land-Use Impacts on Bank Erosion and Deposition of an Incised Stream in North-Central Iowa, Usa. *CATENA*, **125**, 61-73. https://doi.org/10.1016/j.catena.2014.09.013

[40] Camporeale, C., Perucca, E., Ridolfi, L. and Gurnell, A.M. (2013) Modeling the Interactions between River Morphodynamics and Riparian Vegetation. *Reviews of Geophysics*, **51**, 379-414. https://doi.org/10.1002/rog.20014

[41] Wynants, M. (2020) Assessing the Dynamics of Soil Erosion and Sediment Transport Under Increasing Land Use Pressures in East African Rift Catchments. Ph.D. Thesis, University of Plymouth.

[42] Williams, R.D., Measures, R., Hicks, D.M. and Brasington, J. (2016) Assessment of a Numerical Model to Reproduce Event-scale Erosion and Deposition Distributions in a Braided River. *Water Resources Research*, **52**, 6621-6642. https://doi.org/10.1002/2015wr018491

[43] Kocsis, I., Bilaşco, Ş., Irimuş, I., Dohotar, V., Rusu, R. and Roşca, S. (2022) Flash Flood Vulnerability Mapping Based on FFPI Using GIS Spatial Analysis Case Study: Valea Rea Catchment Area, Romania. *Sensors*, **22**, Article 3573. https://doi.org/10.3390/s22093573

[44] Olang, L.O. and Fürst, J. (2010) Effects of Land Cover Change on Flood Peak Discharges and Runoff Volumes: Model Estimates for the Nyando River Basin, Kenya. *Hydrological Processes*, **25**, 80-89. https://doi.org/10.1002/hyp.7821

[45] Das, S. and Pardeshi, S.D. (2018) Morphometric Analysis of Vaitarna and Ulhas River Basins, Maharashtra, India: Using Geospatial Techniques. *Applied Water Science*, **8**, Article No. 158. https://doi.org/10.1007/s13201-018-0801-z

[46] Di Baldassarre, G. (2012) Floods in a Changing Climate: Inundation Modelling. Cambridge University Press. https://doi.org/10.1017/cbo9781139088411

[47] Rwanda Environment Management Authority (2025) Rwanda State of Environment and Outlook Report. https://www.rema.gov.rw/soe/

[48] National Institute of Statistics of Rwanda (2020) Rwanda Statistical Yearbook. Republic of Rwanda. http://www.statistics.gov.rw

[49] Onu, G. and Ngwube, A. (2024) Political Leadership, Corruption and Development in Burundi. *African Renaissance*, No. SI2, 127-148.

[50] Achu, N. (2011) Rwanda and The Nile Cooperative Framework Agreement: Assessing the 1929 Nile Treaty. In: Adar, K.G. and Check, Eds., *Cooperative Diplomacy, Regional Stability and National Interests: The Nile River and the Riparian States*, Africa Inst of South Africa, 85.

[51] Richetta, C. (2015) Land Use Changes and Socio-Political Order in Contemporary Sub-Saharan Africa: Local Effects on Social Trust and Violence. PhD Thesis, Université de Genève.

[52] Huggins, C. (2010) Land, Power and Identity: Roots of Violent Conflict in Eastern DRC. https://www.international-alert.org/publications/land-power-and-identity/

[53] Pritchard, M.F. (2013) Land, Power and Peace: Tenure Formalization, Agricultural Reform, and Livelihood Insecurity in Rural Rwanda. *Land Use Policy*, **30**, 186-196. https://doi.org/10.1016/j.landusepol.2012.03.012